



Reduction of calcium flux from the extracellular region and endoplasmic reticulum by amorphous nano-silica particles owing to carboxy group addition on their surface



Akira Onodera^{a,*}, Katsutoshi Yayama^a, Hideto Morosawa^a, Yukina Ishii^a, Yasuo Tsutsumi^b, Yuichi Kawai^a

^a Department of Pharmaceutical Sciences, Kobegakuin University, 1-1-3 Minatojima, Chuo-ku, Kobe 650-8586, Japan

^b Department of Toxicology, Graduate School of Pharmaceutical Sciences, Osaka University, 1-6 Yamada-oka, Suita, Osaka 565-0871, Japan

ARTICLE INFO

Keywords:

Calcium homeostasis
Nanomaterial
Surface properties

ABSTRACT

Several studies have reported that amorphous nano-silica particles (nano-SPs) modulate calcium flux, although the mechanism remains incompletely understood. We thus analyzed the relationship between calcium flux and particle surface properties and determined the calcium flux route. Treatment of Balb/c 3T3 fibroblasts with nano-SPs with a diameter of 70 nm (nSP70) increased cytosolic calcium concentration, but that with SPs with a diameter of 300 or 1000 nm did not. Surface modification of nSP70 with a carboxy group also did not modulate calcium flux. Pretreatment with a general calcium entry blocker almost completely suppressed calcium flux by nSP70. Preconditioning by emptying the endoplasmic reticulum (ER) calcium stores slightly suppressed calcium flux by nSP70. These results indicate that nSP70 mainly modulates calcium flux across plasma membrane calcium channels, with subsequent activation of the ER calcium pump, and that the potential of calcium flux by nano-SPs is determined by the particle surface charge.

1. Introduction

Nanomaterials (NMs) have superior mechanical and optical properties, which result in increased material strength and color changes according to particle size, respectively. One of the main reasons for the peculiar biological responses to NMs is the fact that their superior physicochemical properties enhance catalytic reactions, caused by an increase in surface area [1].

NMs with the abovementioned properties were found to increase the cytosolic calcium concentration regardless of whether they were composed of organic or inorganic matter [2–5]. NMs composed of organic matter are primarily used for the development of liposomal formulations, namely, microparticles composed of phospholipids or phospholipid analogues. In an analysis of 1,2-distearoyl-sn-glycero-3-phosphoethanolamine-N-[amino(polyethylene glycol)-2000] (PEG2000-DSPE), the treatment of the human lung adenocarcinoma epithelial cell line A549 with this molecule at 35 μ M for 48 h increased the cytosolic calcium concentration by 1.8 times [2]. The suggested underlying mechanism was that PEG2000-DSPE accumulates in the

endoplasmic reticulum (ER) and damages it. The calcium in the ER then leaks into the cytoplasm [2]. In addition, the treatment of hippocampal slices with polyamidoamine generation 5 (G5-NH₂) dendrimer (0.1 mg/mL for 30 min) also increased the cytosolic calcium concentration in the astroglia-rich area [3]. The suggested underlying mechanism was that mitochondrial calcium leakage into the cytoplasm is caused by the G5-NH₂ dendrimer acting on the cell membrane, which consecutively induces mitochondrial polarization [3].

For NMs composed of organic matter, it was also shown that various NMs are associated with calcium homeostasis, and amorphous nano-silica particles (nano-SPs) increased the cytosolic calcium concentration [4,5]. Treatment of GT1-7 neuronal cells with amorphous nano-SPs with a diameter of 50 nm increased the cytosolic calcium concentration from a few minutes after treatment; the cytosolic calcium concentration then decreased to baseline at 4 h [4,5]. The same study suggested that an increase in cytosolic calcium concentration by nano-SPs was suppressed by an inhibitor of L- and T-type voltage-dependent calcium channels and transient receptor potential vanilloid-type channels [4,5]. However, the reactivity of calcium home-

Abbreviations: SP, amorphous silica particle; nano-SP, amorphous nano-silica particle; Balb/3T3, Balb/c 3T3 fibroblast; nSP70, nano-silica particle with a diameter of 70 nm; nSP300, nano-silica particle with a diameter of 300 nm; mSP1000, micro-silica particle with a diameter of 1000 nm; NM, nanomaterial; ER, endoplasmic reticulum; VDCC, voltage-dependent calcium channel.

* Corresponding author.

E-mail address: onodera@pharm.kobegakuin.ac.jp (A. Onodera).

<http://dx.doi.org/10.1016/j.bbrep.2017.01.014>

Received 26 August 2016; Received in revised form 25 January 2017; Accepted 26 January 2017

Available online 04 February 2017

2405-5808/ © 2017 The Authors. Published by Elsevier B.V.

This is an open access article under the CC BY-NC-ND license (<http://creativecommons.org/licenses/by-nc-nd/4.0/>).

ostasis to nano-SPs and the efficacy of inhibition depended on the cell type [4,5]. In addition, regardless of the type of NM, including quantum dots, silver nano-particles, and nano-zinc oxide, increases in cytosolic calcium concentration in the neurons have been reported [6–11].

For neurons, calcium ions act as secondary messengers, regulate the transmission of depolarizing signals, and contribute to synaptic activity [12,13]. Neuronal calcium homeostasis is maintained by flux across the plasma membrane, mitochondria, and ER through channels and receptors. Alzheimer's disease is representative of a disease due to calcium homeostasis failure. Early-onset familial Alzheimer's disease (eFAD) is associated with presenilin-1 (PS1), an integral membrane protein that is primarily localized in the ER; mutations in PS1 are observed in 30–70% of cases [14]. PS1 gene mutation causes an increase in the ER calcium pool and also enhances calcium release through the inositol 1,4,5-trisphosphate and ryanodine receptors. Amyloid accumulation and interference of normal impulse transmission in eFAD are thought to be caused by excessive calcium signaling in synaptic terminals by enhanced calcium flux across the ER [13–15]. Such an enhancement in calcium flux is related to cell death not only in the neurons but also in other cells [16,17]. Upon treating liver parenchymal cells with ATP, it was shown that calcium flux was enhanced by disintegration of the mitochondrial membrane, which subsequently induced cell death [16]. The glucocorticoid induces a sustained increase in cytosolic calcium concentration, which induces the activation of endonuclease with subsequent DNA fragmentation and cell death [17,18].

Some evidence has shown that the onset of toxicity due to different kinds of NP also induces calcium flux [2–5]. However, the types of particle that induce calcium flux remain unclear. We thus analyzed the relationship among particle size, surface charge properties, and calcium flux.

2. Materials and methods

2.1. Cell culture

Cryopreserved mouse BALB/c 3T3 fibroblasts (Balb/3T3) were obtained from the RIKEN Bioresource Center. The cells were thawed and used for experiments after various periods. They were maintained in a state of continuous subconfluent growth by subculturing three times per week using trypsin. They were cultured in Eagle's minimum essential medium (Wako Chemical, Tokyo, Japan) containing 5% fetal calf serum (FCS) at 37 °C in a humidified atmosphere of 5% CO₂ in air.

2.2. Amorphous silica particles

We purchased amorphous nano-SPs with a diameter of 70 nm designated as nSP70 (Sicstar® 43-00-701), nSP70 with carboxylic acid groups (COOH) on the surface designated as nSP70-COOH (Sicstar® 43-02-701), amorphous SPs with a diameter of 300 nm designated as nSP300 (Sicstar® 43-00-302) and amorphous SPs with a diameter of 1000 nm designated as mSP1000 (Sicstar® 43-00-103) from Micromod (Rostock, Germany). These amorphous SPs are nonporous, and the dispersion liquid did not include a surface-active agent. These amorphous SPs were suspended in Hank's balanced salt solution without calcium/magnesium or phenol (HBSS, Wako Chemical 085-09355, Tokyo, Japan), sonicated for 5 min and vortexed for 5 min before use.

2.3. Physicochemical examination of amorphous SPs

To prepare a sample solution with 33.3 µg/mL of amorphous SP, dispersed amorphous SP solution was diluted in cell culture media containing 5% FCS (33.3 µg/mL) and vortexed for 1 min. The average particle size and zeta potential were both measured at room tempera-

ture using a Zetasizer Nano-ZS (Malvern Instruments Ltd, Worcestershire, UK). Particle size distributions were evaluated using dynamic light scattering. The zeta potential was evaluated with dynamic laser Doppler electrophoresis.

2.4. Cell cytotoxicity assay

The cytotoxicity of amorphous SPs was determined using a WST-1 assay (Takara, Tokyo, Japan). This is a method to evaluate viable cells by enzymatic cleavage of the tetrazolium salt WST-1 to formazan by mitochondrial dehydrogenases expressed by viable cells. Balb/3T3 was seeded at 2×10⁴ cells/well (48-well plate) in the culture medium. After incubation for 24 h, the culture supernatant was removed, and the SPs or an equal volume of HBSS was treated in culture media (the final concentration of FCS was around 5%). The SP treatment conditions were 11, 33.3, 100, and 300 µg/mL for 24 h. WST-1 mixtures were added to each well and incubated for 2 h at 37 °C in a humidified atmosphere of 5% CO₂ in air. After incubation, 100 µL of the cell culture supernatant, including WST formazan, was transferred to a 96-well plate, and the absorbance was measured using a microplate reader (ChroMate®, Awareness Technology Inc. Florida, USA) at a wavelength of 450 nm.

2.5. Determination of the cytosolic calcium concentration

The ability of nano-SPs to modulate calcium flux was determined using a Fluo 4-acetoxymethyl ester assay (Fluo 4-AM, F312; Dojindo Laboratories, Kumamoto, Japan). This is a method used to evaluate the cytosolic concentration of calcium ions, in which the nonfluorescent acetoxymethyl Fluo 4-AM is cleaved by intracellular esterase to form free green fluorescent Fluo 4, which is a calcium indicator. When it forms a complex with calcium, excitation by light at a wavelength of 488 nm produces marked green fluorescence inside the cell. In this experiment, Balb/3T3 cells were seeded at 2×10³ cells/well (in glass-bottomed culture dishes; Matsunami Glass Ind. Ltd. Osaka, Japan) in the culture medium. After incubation for 24 h, the cells were pretreated with Fluo-4 AM mixture in accordance with the attached protocol from Dojindo Laboratories. The intensity of intracellular green fluorescence in live cells was observed from 1 min before treatment until 20 min after treatment with ATP or SPs using a FluoView FV1000 confocal laser scanning microscope (Olympus, Tokyo, Japan) at room temperature in an air-conditioned laboratory. ATP and SPs were applied at concentrations of 100 µM and 300 µg/mL, respectively. Vehicle control cells received an equal volume of HBSS. In some experiments, the inhibitor SKF96365 (SKF; 10 µM) or thapsigargin (Thap; 2 µM) was added 2 h before the addition of nSP70. Cells were imaged using an inverted microscope (IX81; Olympus) equipped with a 20× or 40× objective lens. Green fluorescence of Fluo-4 was excited at 473 nm, and emission was detected at 516 nm. Green fluorescence intensity was profiled for the whole cell in approximately 10–20 cells using fv10-asw 2.0 viewer software (Olympus). The intensity of whole-cell fluorescence was plotted for each time point using the equivalent intensity at 1 min before the addition of HBSS, ATP, or SPs as a standard.

2.6. Statistical analysis

The results are expressed as mean ± standard error of mean (SEM). *In vitro* assays were performed in 3–5 independent experiments. Data analysis was performed using analysis of variance (ANOVA) and Tukey's HSD tests with Kaleida Graph statistical software. A *P*-value of < 0.05 or 0.001 was considered statistically significant.

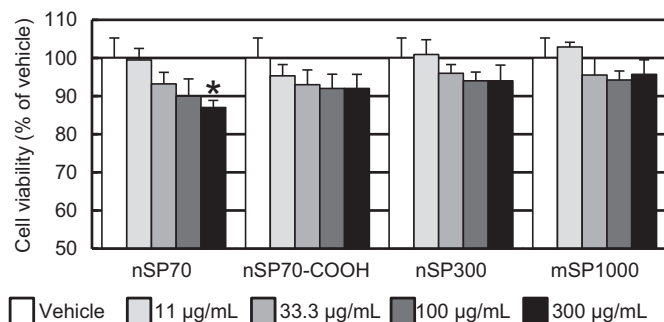
3. Results and discussion

The purpose of the present study was to determine the influence of the surface charge properties of nano-SPs on calcium flux to identify the calcium flux route affected by these particles. Therefore, we used

Table 1

Physicochemical characterization of amorphous silica particle suspensions in HBSS and cell culture media (medium).

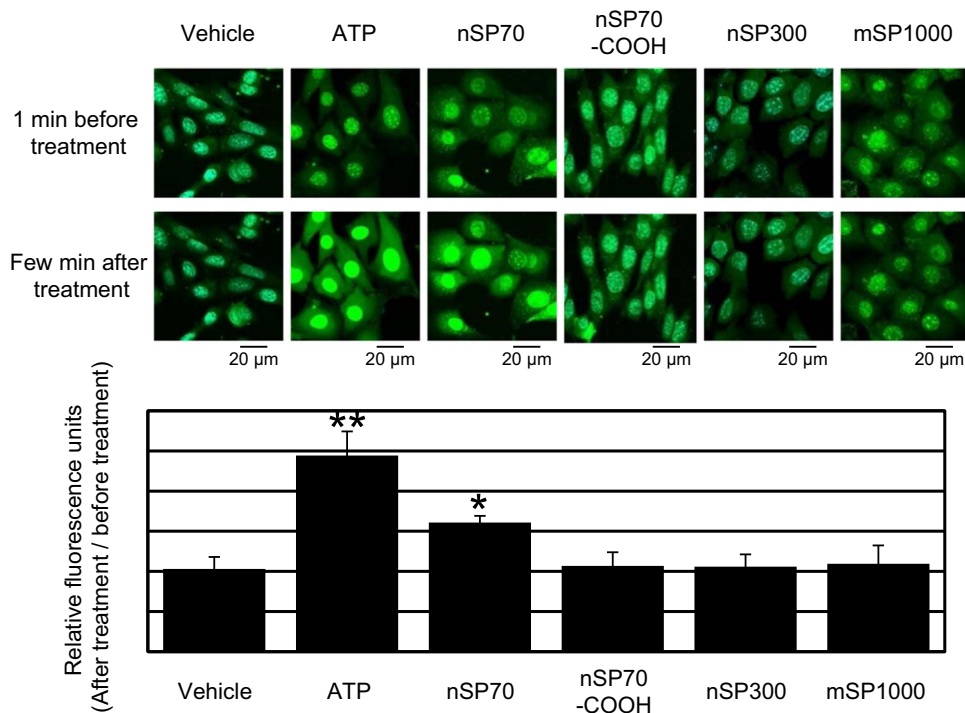
	Solution	Diameter (nm)	Polydispersity index	ζ potential (mV)
nSP70	HBSS	75.9 ± 0.25	0.054 ± 0.043	-25.8 ± 1.25
	Medium	128.4 ± 0.70	0.105 ± 0.018	-11.4 ± 1.03
nSP70-COOH	HBSS	65.47 ± 0.18	0.043 ± 0.02	-28.7 ± 1.31
	Medium	102.6 ± 0.25	0.167 ± 0.004	-18.6 ± 0.64
nSP300	HBSS	383.4 ± 4.14	0.129 ± 0.018	-32.5 ± 1.29
	Medium	501.0 ± 3.27	0.241 ± 0.018	-11.5 ± 0.95
mSP1000	HBSS	999.1 ± 6.85	0.17 ± 0.02	-32.8 ± 1.11
	Medium	1229 ± 147.4	0.197 ± 0.111	-10.9 ± 0.36

**Fig. 1.** Cytotoxicity of amorphous nano-silica particles after 24 h of exposure. The viability of Balb/3T3 was determined using WST-1 assays as described in the Section 2; *P < 0.05 vs. vehicle (ANOVA and Tukey's HSD tests).

four kinds of SP: nanoparticles < 100 nm (nSP70) as NMs, two sizes of microparticle > 100 nm (nSP300 and mSP1000), and surface-modified nanoparticles < 100 nm (nSP70-COOH) in buffer (Table 1). Suspending these amorphous SPs in cell culture media containing FCS increased the particle sizes; the particle diameters of nSP70,

nSP70-COOH, nSP300, and mSP1000 increased from 75 nm, 65 nm, 383 nm, and 999–128 nm, 102 nm, 501 nm, and 1229 nm, respectively (Table 1). The zeta potentials also changed; those of nSP70, nSP300, and mSP1000 became -11 mV, and that of nSP70-COOH became -18.6 mV (Table 1). With respect to the effects of these particles on cell viability, a significant decrease (by 87%) in viability was observed upon treatment with only 300 µg/mL nSP70 for 24 h, but not with nSP300 or mSP1000 (Fig. 1). In addition, upon surface modification of nSP70 with COOH, there was no significant decrease in cell viability (Fig. 1). Previous studies reported that regarding the cytotoxicity of nano-SPs, increases in lactate dehydrogenase release, reactive oxygen species production, and DNA damage by nSP70 were being reduced owing to surface modification with COOH [21]. These results suggest that the effects of nano-SPs on Balb/3T3 are limited in contrast to the results of previous reports [19–21]. Although the cytotoxic effects of nSP70 are weak, COOH modification was effective in reducing cytotoxicity in Balb/3T3, as in a previous report using other cell lines [19–21].

Next, we investigated the effects of these SPs on calcium flux. To confirm the calcium flux responses of Balb/3T3, we determined calcium flux after addition of ATP, which induces a transient rise in cytosolic calcium by transporting calcium from the extracellular region and reflects secondary messenger-operated calcium release from the ER [20]. Note that we have showed the change in intracellular calcium density in relative fluorescence units (RFU). Moreover, RFU were based on the intensity of fluorescence before measurements, and calculated as the maximum intensity of fluorescence observed after measurements for 20 min. The intracellular calcium concentration increased 2.4 times within a few minutes after treatment with ATP (Fig. 2). Next, we analyzed calcium flux due to SPs and its dependence on the particle size and surface charge properties. The treatment of cells with 300 µg/mL nSP70 significantly increased the intracellular calcium concentration by 1.6 times compared with the increase due to treatment with nSP300 or mSP1000 (Fig. 2). Surface modification of nSP70 by the addition of COOH did not increase intracellular calcium,

**Fig. 2.** Calcium flux from ATP, nSP70, nSP70-COOH, nSP300, and mSP1000 in Balb/3T3. To determine the modulation of calcium flux by SPs in Balb/3T3, we performed Fluo-4 assays. The cells were pretreated with the Fluo-4 AM mixture for 30 min. The intensity of intracellular green fluorescence was observed from 1 min before until 20 min after treatment with ATP or SPs. The fluorescence of Fluo-4 is excited at 473 nm, and emission was detected at 516 nm. The assay was performed in 3–5 independent experiments; *P < 0.05 vs. vehicle (ANOVA and Tukey's HSD tests).

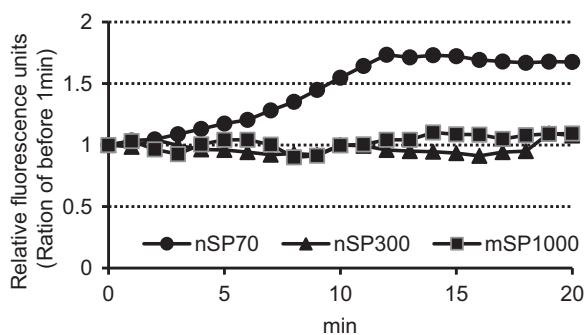


Fig. 3. A typical image showing changes in intracellular calcium concentrations from SPs. Balb/3T3 cells were seeded at 2×10^3 cells/well in culture medium. After incubation for 24 h, the cells were pretreated with the Fluo-4 AM mixture for 30 min. The intensity of intracellular green fluorescence was observed from 1 min before until 20 min after treatment with 300 $\mu\text{g}/\text{mL}$ SP using a FluoView FV1000 confocal laser scanning microscope. The fluorescence of Fluo-4 was excited at 473 nm, and emission was detected at 516 nm. nSP70, closed circle (●); nSP300, closed triangle (▲); and mSP1000, closed square (■). The assay was performed in 3–5 independent experiments.

and RFU for nSP70 decreased from 1.6 to 1.1 (Fig. 2). In addition, the calcium flux from nSP70 was not transient, but maintained the calcium density, which increased from 1.6 to 1.7 times over 20 min when the observations were performed (Fig. 3). With respect to the zeta potential of human cells, that of HeLa cells is -19.4 mV and that of erythrocytes is -31.8 mV [22]. Although the zeta potential depends on the type of cell, it is thought that the zeta potential of Balb/3T3 is negative. Our findings strongly suggest that the interaction between cells and nano-SPs mainly occurs via electrical forces (Figs. 2 and 3).

Here, we also determined the calcium flux route influenced by nSP70. Specifically, we used an ER calcium-ATPase pump inhibitor, Thap, which depletes ER calcium stores, and a non-selective cation channel inhibitor, SKF, which suppresses receptor-mediated and voltage-gated calcium entry from the extracellular region [23,24]. RFU for nSP70 decreased from 1.6 to 1.0 or 1.3 because of Thap or SKF, respectively (Fig. 4). These findings suggest that the major route for calcium flux modulated by nano-SPs is from the extracellular region, whereas calcium release from the ER is secondarily promoted.

It is known that an increase in unintentional calcium flux induces cell death [25,26]. It is thought that nano-SP cytotoxicity is caused by a similar mechanism. Regarding this analysis, the calcium flux from nSP70 was 1.6 times weaker. Although the cell line was different, intracellular calcium density increased by more than 10 times from calcium ionophores used for the purpose of evoking calcium signaling [27]. It is regarded that the weak cytotoxicity of nSP70 was caused by

an increase in the weak calcium flux from nSP70. On one hand, we found that one type of catalytic activity of nano-SPs was the promotion of calcium flux from the extracellular region and the ER. Moreover, we used amorphous nano-SPs with a diameter of 70 nm as a model of the NMs by this analysis; therefore, size-dependent elucidation in particles less than 100 nm will probably be a problem in the future. Wen Jiang et al. clearly indicated that colloidal gold nanoparticles with a diameter of 40–50 nm were most likely to bind to the receptor. Particles more likely to internalize were those with a diameter of 2–100 nm that coupled an antigen [28]. Identification of reacting or binding molecules or proteins in the plasma membrane was different in each type of cell and the underlying mechanism requires a better understanding about calcium flux by NMs. This analysis cannot determine the electrochemical interaction that specifies what kind of reaction takes place between a cell membrane and a particle.

4. Conclusion

The calcium flux and cytotoxicity of nSP70 were suppressed by changing the surface charge property to negative; the intensity of this ability is thought to be determined by particle–surface electrostatic interactions. Through biotechnological assays, this report cannot demonstrate the electrochemical interaction of a cell membrane and the nanoparticle. Using molecular dynamic stimulation, Kenta Shimizu et al. showed that anionic gold nanoparticles translocate across the cell membrane. This does not occur with anionic and neutral gold nanoparticles, a finding that improves appropriateness and credibility of our results and discussions [29]. The present study suggests that the safety of NMs can be dramatically improved by modifying the particle surface.

Acknowledgments

This study was supported in part by a Grant-in-Aid for Young Scientists (B), Health Labour Sciences Research Grants from the Ministry of Health, Labour and Welfare of Japan (MHLW), the Japan Food Chemical Research Foundation, the Program for the Strategic Research Foundation at Private Universities (S1201010), and Kobegakuin University Grant C.

Appendix A. Transparency document

Transparency document associated with this article can be found in the online version at <http://dx.doi.org/10.1016/j.bbrep.2017.01.014>.

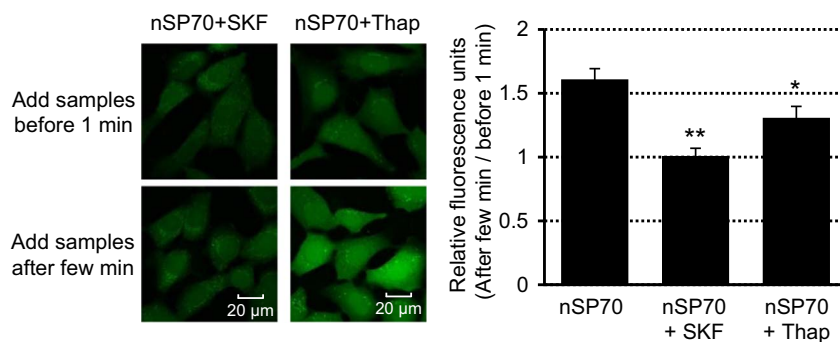


Fig. 4. Determination of the underlying mechanism of promotion of calcium flux by nSP70. To determine the mechanism by which nSP70 promotes calcium flux, we analyzed the effects of a calcium channel or pump inhibitor, SKF96365 (SKF) or thapsigargin (Thap), on calcium flux. The cells were pretreated with each inhibitor for 2 h. They were then treated with Fluo-4 AM mixture for 30 min before the addition of nSP70. The intensity of intracellular green fluorescence was observed from 1 min before until 20 min after treatment with nSP70. Fluorescence of Fluo-4 was excited at 473 nm and emission was detected at 516 nm. The assay was performed in 3–5 independent experiments; * $P < 0.05$ vs. nSP70; ** $P < 0.001$ vs. nSP70 (ANOVA and Tukey's HSD tests).

References

- [1] S. Chaturvedi, P.N. Dave, N.K. Shah, Applications of nano-catalyst in new era, *J. Saudi Chem. Soc.* 16 (2012) 307–325.
- [2] J. Wang, X. Fang, W. Liang, Pegylated phospholipid micelles induce endoplasmic reticulum-dependent apoptosis of cancer cells but not normal cells, *ACS Nano* 6 (2012) 5018–5030.
- [3] L. Nyitrai, I. Héja, I. Jablonkai, et al., Polyamidoamine dendrimer impairs mitochondrial oxidation in brain tissue, *J. Nanobiotechnology* 11 (2013) 9.
- [4] P. Ariano, P. Zamburlin, A. Gilardino, et al., Interaction of spherical silica nanoparticles with neuronal cells: size-dependent toxicity and perturbation of calcium homeostasis, *Small* 7 (2011) 766–774.
- [5] A. Gilardino, F. Catalano, F.A. Ruffinatti, et al., Interaction of SiO₂ nanoparticles with neuronal cells: ionic mechanisms involved in the perturbation of calcium homeostasis, *Int. J. Biochem. Cell Biol.* 66 (2015) 101–111.
- [6] M. Tang, T. Xing, J. Zeng, et al., Unmodified CdSe quantum dots induce elevation of cytoplasmic calcium levels and impairment of functional properties of sodium channels in rat primary cultured hippocampal neurons, *Environ. Health Perspect.* 116 (2008) 915–922.
- [7] M.I. Tang, M. Wang, T. Xing, et al., Mechanisms of unmodified CdSe quantum dot-induced elevation of cytoplasmic calcium levels in primary cultures of rat hippocampal neurons, *Biomaterials* 29 (2008) 4383–4391.
- [8] N. Yin, Q. Liu, J. Liu, et al., Silver nanoparticle exposure attenuates the viability of rat cerebellum granule cells through apoptosis coupled to oxidative stress, *Small* 9 (2013) 1831–1841.
- [9] A. Haase, S. Rott, A. Manton, et al., Effects of silver nanoparticles on primary mixed neural cell cultures: uptake, oxidative stress and acute calcium responses, *Toxicol. Sci.* 126 (2012) 457–468.
- [10] D. Guo, H. Bi, D. Wang, et al., Zinc oxide nanoparticles decrease the expression and activity of plasma membrane calcium ATPase, disrupt the intracellular calcium homeostasis in rat retinal ganglion cells, *Int. J. Biochem. Cell Biol.* 45 (2013) 1849–1859.
- [11] H.J. Wang, A.C. Growcock, T.H. Tang, et al., Zinc oxide nanoparticle disruption of store-operated calcium entry in a muscarinic receptor signalling pathway, *Toxicol. In Vitro* 24 (2010) 1953–1961.
- [12] C. Grienberger, A. Konnerth, Imaging calcium in neurons, *Neuron* 73 (2012) 862–885.
- [13] M. Brini, T. Cali, D. Ottolini, et al., Neuronal calcium signalling: function and dysfunction, *Cell Mol. Life Sci.* 71 (2014) 2787–2814.
- [14] M.R. Cornejo-Olivas, C.E. Yu, P. Mazzetti, et al., Clinical and molecular studies reveal a PSEN1 mutation (L153V) in a Peruvian family with early-onset Alzheimer's disease, *Neurosci. Lett.* 563 (2014) 140–143.
- [15] M.P. Mattson, ER calcium and Alzheimer's disease: in a state of flux, *Sci. Signal.* 3 (2010) (pe10).
- [16] J.P. Zoetewij, B. Water, H.J. Bont, et al., Calcium-induced cytotoxicity in hepatocytes after exposure to extracellular ATP is dependent on inorganic phosphate. Effects on mitochondrial calcium, *J. Biol. Chem.* 268 (1993) 3384–3388.
- [17] J.J. Cohen, R.C. Duke, Glucocorticoid activation of a calcium-dependent endonuclease in thymocyte nuclei leads to cell death, *J. Immunol.* 132 (1984) 38–42.
- [18] D.J. McConkey, P. Nicotera, P. Hartzell, et al., Glucocorticoids activate a suicide process in thymocytes through an elevation of cytosolic calcium concentration, *Arch. Biochem. Biophys.* 269 (1989) 365–370.
- [19] H. Nabeshi, T. Yoshikawa, K. Matsuyama, et al., Size-dependent cytotoxic effects of amorphous silica nanoparticles on Langerhans cells, *Pharmazie* 65 (2010) 199–201.
- [20] S.R. Alonso-Torre, A. Trautmann, Calcium responses elicited by nucleotides in macrophages. Interaction between two receptor subtypes, *J. Biol. Chem.* 268 (1993) 18640–18647.
- [21] T. Yoshida, Y. Yoshioka, K. Matsuyama, et al., Surface modification of amorphous nanosilica particles suppresses nanosilica-induced cytotoxicity, ROS generation, and DNA damage in various mammalian cells, *Biochem. Biophys. Res. Commun.* 427 (2012) 748–752.
- [22] O.V. Bondar, D.V. Saifullina, I.I. Shakhmaeva, et al., Monitoring of the zeta potential of human cells upon reduction in their viability and interaction with polymers, *Acta Nat.* 4 (2012) 78–81.
- [23] J. Lytton, M. Westlin, M.R. Hanley, Thapsigargin inhibits the sarcoplasmic or endoplasmic reticulum Ca-ATPase family of calcium pumps, *J. Biol. Chem.* 266 (1991) 17067–17071.
- [24] T. Chen, J. Zhu, C. Zhang, et al., Protective effects of SKF-96365, a non-specific inhibitor of SOCE, against MPP⁺-induced cytotoxicity in PC12 cells: potential role of Homer1, *PLoS One* 8 (2013) e55601.
- [25] J. Wang, J. Yang, P. Liu, et al., NAD induces astrocyte calcium flux and cell death by ART2 and P2×7 pathway, *Am. J. Pathol.* 181 (2012) 746–752.
- [26] E. Jambriña, R. Alonso, M. Alcalde, et al., Calcium influx through receptor-operated channel induces mitochondria-triggered paraptotic cell death, *J. Biol. Chem.* 278 (2013) 14134–14145.
- [27] T.J. Rink, S.W. Smith, R.Y. Tsien, Cytoplasmic free Ca²⁺ in human platelets: Ca²⁺ thresholds and Ca-independent activation for shape-change and secretion, *FEBS Lett.* 148 (1982) 21–26.
- [28] W. Jiang, B.Y. Kim, J.T. Rutka, et al., Nanoparticle-mediated cellular response is size-dependent, *Nat. Nanotechnol.* 3 (2008) 145–150.
- [29] K. Shimizu, H. Nakamura, et al., MD simulation study of direct permeation of a nanoparticle across the cell membrane under an external electric field, *Nanoscale* 8 (2016) 11897–11906.